

Validation of the Practicability of Logical Assessment Formula for Evaluations with Inaccurate Ground-Truth Labels

Yongquan Yang¹ and Hong Bu^{1,2}

1. Institute of Clinical Pathology, West China Hospital, Sichuan University, Chengdu, China. Email: remy_yang@foxmail.com

2. Department of Pathology, West China Hospital, Sichuan University, Chengdu, China. Email: hongbu@scu.edu.cn

Abstract

Logical assessment formula (LAF) is a new theory proposed for evaluations with inaccurate ground-truth labels (IAGTLs) to assess the predictive models for various artificial intelligence applications. However, the practicability of LAF for evaluations with IAGTLs has not yet been validated in real-world practice. In this paper, to address this issue, we applied LAF to tumour segmentation for breast cancer (TSfBC) in medical histopathology whole slide image analysis (MHWSIA). Experimental results and analysis show the validity of LAF for evaluations with IAGTLs in the case of TSfBC and reflect the potentials of LAF applied to MHWSIA.

1. Introduction

Logical assessment formula (LAF) [1] was proposed to achieve evaluations with inaccurate ground-truth labels (IAGTLs), which alleviates the usual evaluations with accurate ground-truth labels (AGTLs) [2–6], to assess predictive models for various artificial intelligence applications. LAF is suitable for evaluating the predicted targets of a predictive model in the situation, where the underlying true targets are difficult to be precisely defined while multiple inaccurate targets that contain various information consistent with our prior knowledge about the underlying true target are available. Theoretical analysis of LAF revealed the practicability of LAF for evaluations with IAGTLs, which includes: 1) LAF can be applied for evaluations with IAGTLs on a more difficult task, able to act like usual strategies for evaluations with AGTLs reasonably; and 2) LAF can be applied for evaluations with IAGTLs simply from the logical point of view on an easier task, unable to act like usual strategies for evaluations with AGTLs confidently.

However, the revealed practicability of LAF for evaluations with IAGTLs has not yet been validated in real-world practice. In this paper, we aimed to address this issue. We applied LAF to tumour segmentation for breast cancer (TSfBC) in medical histopathology whole slide image analysis (MHWSIA). Extensive experiments were conducted and corresponding results and analyses support that the practicability of LAF is valid in the case of TSfBC in MHWSIA, which reflect the potentials of LAF applied to MHWSIA for evaluations with IAGTLs.

The rest contents of this paper are structured as follows. In Section 2, we briefly review LAF. In Section 3, we give the details of the implementation of LAF applied to TSfBC in MHWSIA. In Section 4, we conduct extensive experiments and analyse corresponding results to validate the practicability of LAF in the case of TSfBC in MHWSIA. Finally, we conclude and discuss the whole paper in Section 5.

2. Preliminary of Logical Assessment Formula

Logical assessment formula (LAF) constitutes of three processing procedures, including logical fact narration, logical consistency estimation and logical assessment metric build. The logical fact narration procedure narrates a list of logical facts about the underlying true targets from the multiple inaccurate targets. The logical consistency estimation procedure estimates a list of logical consistencies between the predicted targets and the logical facts about the underlying true targets narrated by the logical fact narration procedure. The logical assessment metric build procedure derives a series of abstractly formalized metrics from the logical consistencies estimated by the logical consistency estimation procedure to represent the evaluations of the predicted targets compared with the underlying true targets. More details of LAF and its principles are provided at [1].

2.1. Formation and usage of LAF

The formation of LAF can be formally denoted as

$$LAF \left\{ \begin{array}{l} \text{inputs: } \{\tilde{t} = \{\tilde{t}_1, \dots, \tilde{t}_m\}\} \\ PC \left\{ \begin{array}{l} LF = \text{LogicalFactNarrate}(\tilde{t}; p^{LFN}) \\ LC = \text{LogicalConsistencyEstimate}(t, LF; p^{LCE}) \\ LAM = \text{LogicalAssessmentMetricBuild}(LC; p^{LAM}) \end{array} \right. \\ \text{output: } LAM = \{LAM_1, \dots, LAM_w\} \end{array} \right. \quad (1)$$

Specifically, given the predicted target (t) for the underlying true targets which are difficult to be precisely defined and multiple inaccurate targets (\tilde{t}) that contain various information consistent with our prior knowledge about the underlying true target, we can obtain, via the processing components of LAF ($LAF:PC$), a series of logical assessment metrics (LAM) for evaluations of the given predicted target (t) compared with the underlying true target. Formally, the usage of LAF can be denoted as

$$\begin{aligned} LAM &= LAF:PC(t, \tilde{t}; \{p^{LFN}, p^{LCE}, p^{LAM}\}) \\ &= \{LAM_1, \dots, LAM_w\}. \end{aligned} \quad (2)$$

Each p^* of expressions (2) denotes the hyper-parameters corresponding to the implementation of respective expression of $LAF:PC$.

2.2. LAF-based method performance evaluation

LAF-based method performance evaluation (LAF-MPE) strategy is to estimate the effectiveness of a method for addressing a task. As the method and the task should be specifically given in advance, LAF-MPE is task specific (ts) and method specific (ms). The input of LAF-MPE is a series of task specific and method specific logical

assessment metrics ($LAM_{ts,ms}$). The output of LAF-MPE is some method performances ($LMP_{ts,ms}$), which are respectively quantized in range $[0,1]$, to reflect the superiorities of the given specific method for addressing a specific task. As a result, the processing component (PC) of LAF-MPE can be formally expressed as

$$\begin{aligned} LMP_{ts,ms} &= LogicalMethodPerfEval(LAM_{ts,ms}; p^{LMPE}) \\ &= \{LMP_{ts,ms,1}, \dots, LMP_{ts,ms,v}\}, Val(LMP_{ts,ms,v}) \in [0,1]. \end{aligned} \quad (8)$$

Here, p^{LMPE} denotes the hyper-parameters for implementation of formula (8) and $Val(*)$ denotes the value of $*$.

2.3. Practicability of LAF

The practicability of LAF is as follows:

Practicability 1. LAF can be applied for evaluations with IAGTLs on a more difficult task, able to act like usual strategies for evaluations with AGTLs reasonably.

Practicability 2. LAF can be applied for evaluations with IAGTLs simply from the logical point of view on an easier task, unable to act like usual strategies for evaluations with AGTLs confidently.

3. LAF Applied to Tumour Segmentation for Breast Cancer

In this section, we apply LAF to two tasks of tumour segmentation for breast cancer (TSfBC) in medical histopathology whole slide image analysis (MHWSIA) for evaluations with inaccurate ground-truth labels (IAGTLs). In section 3.1, we briefly describe the two tasks of TSfBC. In section 3.2, we give descriptions about the settings for the application of LAF to TSfBC. In section 3.3, we provide the details of the implementations of LAF applied to TSfBC.

3.1. Tumour segmentation for breast cancer

The two tasks of TSfBC include a task that aims to segment tumour in HE-stained pre-treatment biopsy images and a task that aims to segment residual tumour in HE-stained post-treatment surgical resection images. It is indeed difficult to accurately annotate the true targets for both tasks. Referring to additional suggestions from pathology experts, we here claim that the tumour segmentation task in HE-stained post-treatment surgical resection images is more difficult than the tumour segmentation task in HE-stained pre-treatment biopsy images. More details about the two tasks of TSfBC are available at [7].

3.2. Application settings

Since our main purpose in this application is to apply LAF to the two tasks of TSfBC for evaluations with IAGTLs, we focus more on the settings required by LAF instead of the details of the specific methods for addressing the two tasks.

3.2.1 Inputs of LAF

The outline of the inputs of LAF applied to TSfBC is shown as Fig. 1. Due to the fact that the underlying true targets for the two tasks of TSfBC are difficult to be precisely defined, we set up the two tasks as problems of learning from inaccurate

(noisy) labels [8,9]. Testing samples with IAGTLs provided by pathology experts for the two tasks of TSfBC are shown as the middle of Fig. 1. In the middle of Fig. 1, IAGTLs(1) include many non-tumour areas as tumour areas while IAGTLs(2) exclude many tumour areas as non-tumour areas, which indicates that preparing IAGTLs require much less labour. Two types of inaccurate targets corresponding to the testing samples are extracted from the given IAGTLs via one-step abductive logical reasoning [7,10]. Examples of the extracted two types of inaccurate targets corresponding to the testing samples are shown as the left of Fig. 1. The predicted targets corresponding to the testing samples are obtained via image semantic segmentation model trained with methods for learning from inaccurate labels, which will be discussed later in section 3.2.2-3. Examples of the predicted targets corresponding to the testing samples are shown as the right of Fig. 1.

Note, here, although we omitted the details of extracting the two types of inaccurate targets since our main purpose in this section is to implement the application of LAF to TSfBC for evaluations with IAGTLs, we claim that the extracted two types of inaccurate targets contain information consistent with our prior knowledge about the underlying true targets according to one-step abductive logical reasoning. More specifically, the extracted targets (1) ($\tilde{t}_{TSfBC,1}$) can keep high recall of the underlying true targets of TSfBC and the extracted targets (2) ($\tilde{t}_{TSfBC,2}$) can keep high precision of the underlying true targets of TSfBC. As a result, we denote the multiple inaccurate targets that contain various information consistent with our prior knowledge about the underlying true targets of TSfBC by

$$\tilde{t}_{TSfBC} = \{\tilde{t}_{TSfBC,1}, \tilde{t}_{TSfBC,2}\}.$$

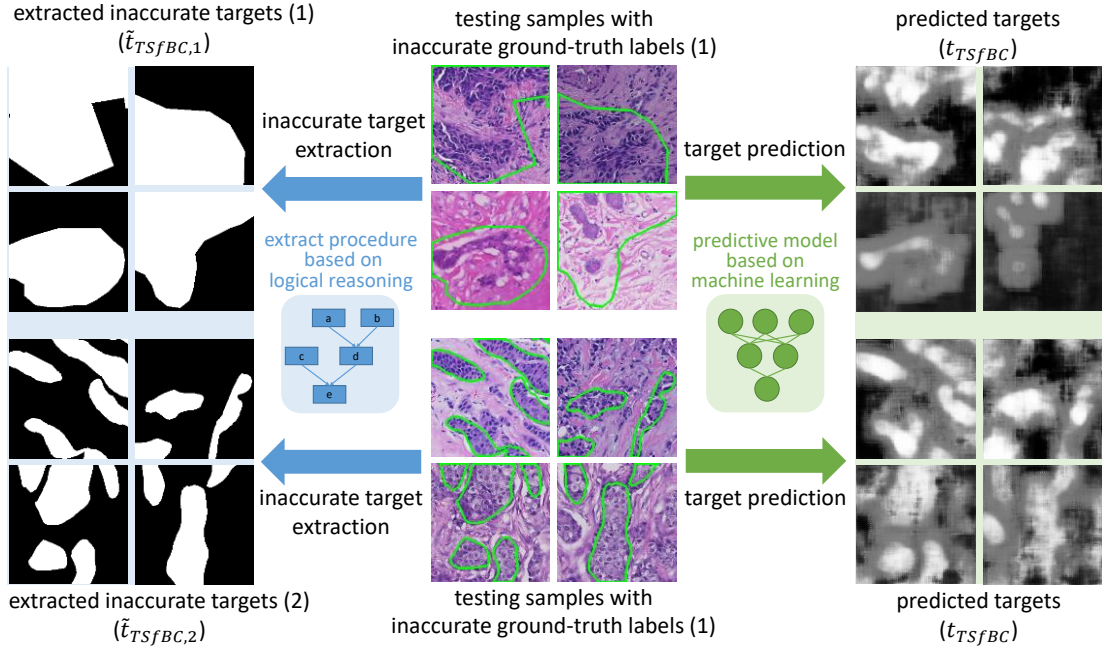


Figure. 3. Outline of the settings for the inputs of LAF applied to TSfBC. Middle: testing samples with inaccurate ground-truth labels (IAGTLs); Left: inaccurate targets corresponding to testing samples; Right: predicted targets corresponding to testing samples.

3.2.2 Image semantic segmentation model

The base image semantic segmentation model (ISSM) for the predicted targets corresponding to the testing samples for the two tasks of TSfBC is a symmetric deep convolutional neural network (DCNN) that was built for the task of H. pylori segmentation [10]. We let $\{cnn_l\}_{l=0}^X$ denote the transformation for each of the X layers from the built base DCNN, $\{w_l\}_{l=0}^X$ denote the parameters of $\{cnn_l\}_{l=0}^X$, and p^{DCNN} denote the hyperparameters for the optimization of $\{w_l\}_{l=0}^X$. We assume that the input of the built base DCNN (an image instance) is I and the output of the built base DCNN (a predicted target corresponding to the input image instance I) is t_{TSfBC} . With all these denotations and assumptions, we can express the image semantic segmentation model (ISSM) for the two tasks of TSfBC by

$$t_{TSfBC} = ISSM(I; \{DCNN, p^{DCNN}\}),$$

$$DCNN = \{\{cnn_l\}_{l=0}^X, \{w_l\}_{l=0}^X\}.$$

Note, in practice, p^{DCNN} can be a designated method of learning from inaccurate labels based on deep learning, since we set up the two tasks of TSfBC as problems of learning from noisy labels.

3.2.3 Methods of learning from inaccurate labels

In addition to the baseline method (BaseLine) that directly learns from the inaccurate labels, various state-of-the-art methods for learning from inaccurate labels, including Forward, Backward [11], Boost-Hard, Boost-Soft [12,13], D2L [14], SCE [15], Peer [16], DT-Forward [17], and NCE-SCE [18], are also chosen to designate the hyperparameter p^{DCNN} for experimental investigations. These state-of-the-art methods are chosen due to their flexibility to be applied to the situation where no clean dataset is available, the targeted object cannot be precisely defined, and any of the given inaccurate labels cannot be confidently regarded as probably true targets. In addition, these state-of-the-art methods respectively combined with an improved version of one-step abductive multi-target learning (OSAMTL) [7] was also chosen to designate the hyperparameter p^{DCNN} for experimental investigations. We respectively set the hyperparameters of these approaches as suggested by corresponding papers. We denote the designated p^{DCNN} by the method-specific (ms) p_{ms}^{DCNN} . As a result, we rewrite the formulation of the image semantic segmentation model for the two tasks of TSfBC by

$$t_{TSfBC,ms} = ISSM(I; \{DCNN, p_{ms}^{DCNN}\}),$$

$$ms \in \{BaseLine, \dots, NCE - SCE, BaseLine_OSAMTL, \dots, NCE - SCE_OSAMTL\}.$$

3.3. Implementation of LAF applied to TSfBC

On the basis of LAF reviewed in Section 2 and the application settings required by LAF to be carried out, we provide an implementation of LAF suitable to be applied for evaluations with IAGTLs on TSfBC.

3.3.1 Implementation of task-specific LAF

We implement a task-specific LAF that is suitable for evaluations with IAGTL on TSfBC. The outline for the application of LAF to TSfBC is summarized as Fig. 2.

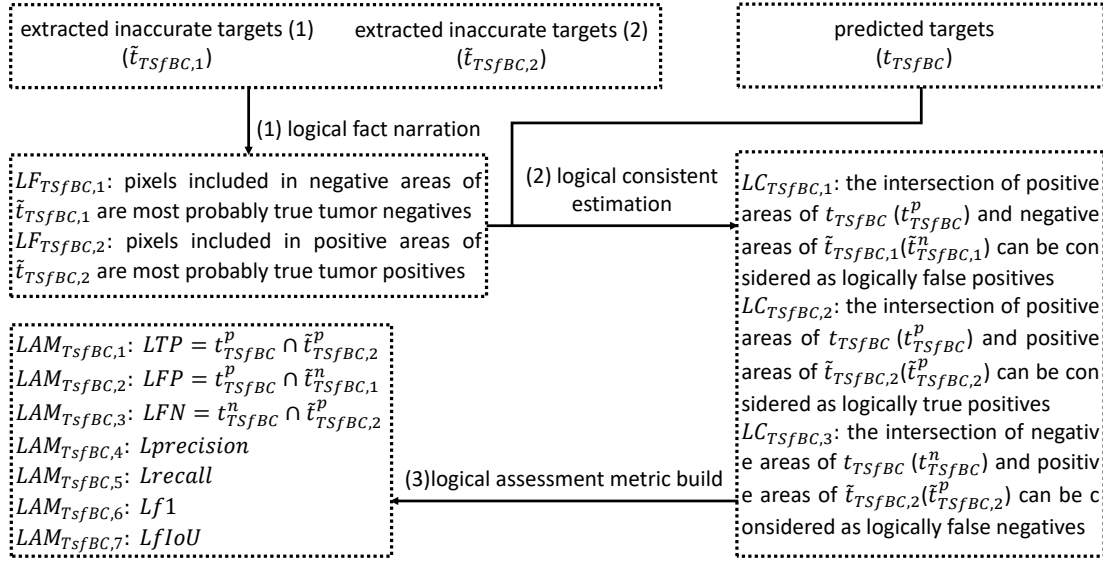


Figure. 2. Outline for the application of LAF to TSfBC.

Referring to formula (4) and letting $ts = TSfBC$ and $m = 2$, we can denote the task-specific LAF that is suitable for evaluations with IAGTL on TSfBC as

$$LAF \begin{cases} inputs: \begin{cases} t_{TSfBC} \\ \tilde{t}_{TSfBC} = \{\tilde{t}_{TSfBC,1}, \tilde{t}_{TSfBC,2}\} \end{cases} \\ PC \begin{cases} LF_{ts} = LogicalFactNarrate(\tilde{t}_{TSfBC}; p_{TSfBC}^{LFN}) \\ LC_{ts} = LogicalConsistencyEstimate(t_{TSfBC}, LF_{TSfBC}; p_{TSfBC}^{LCE}) \\ LAM_{ts} = LogicalAssessmentMetricBuild(LC_{TSfBC}; p_{TSfBC}^{LAM}) \end{cases} \\ outputs: LAM_{TSfBC} \end{cases}$$

We need to clearly define each p_{TSfBC}^* of respective processing component for the implementation of task-specific LAF, regarding to the inherent characteristics of TSfBC.

(1) Logical facts narration

On the basis of the claim that the inaccurate targets $\tilde{t}_{TSfBC} = \{\tilde{t}_{TSfBC,1}, \tilde{t}_{TSfBC,2}\}$ in section 3.2.1 contain information consistent with our prior knowledge about the underlying true target, and the given inaccurate target $\tilde{t}_{TSfBC,1}$ can keep high recall of the underlying true target of TSfBC and the given inaccurate target $\tilde{t}_{TSfBC,2}$ can keep high precision of the underlying true target of TSfBC, we introduce two reasonings (Reasoning 1 and Reasoning 2). The validity of the two derived reasonings are respectively proved by Proof-R1 and Proof-R2 which are provided in Supplementary.

Reasoning 1. If $\tilde{t}_{TSfBC,1}$ is given, then pixels included in negative areas of $\tilde{t}_{TSfBC,1}$ are most probably true tumour negatives.

Reasoning 2. If $\tilde{t}_{TSfBC,2}$ is given, then pixels included in positive areas of $\tilde{t}_{TSfBC,2}$ are most probably true tumour positives.

Referring to Eq. (6) and using Reasoning 1-2 as p_{TSfBC}^{LFN} , we implement the *LogicalFactNarrate*, which narrates two logical facts from \tilde{t}_{TSfBC} , as follows

$$\begin{aligned}
LF_{TSfBC} &= LogicalFactNarrate(\tilde{t}_{TSfBC}; \{Reasoning\ 1, Reasoning\ 2\}) \\
&= \left\{ LogicalFactNarrate(\tilde{t}_{TSfBC,1}; \{Reasoning\ 1\}), \right. \\
&\quad \left. LogicalFactNarrate(\tilde{t}_{TSfBC,2}; \{Reasoning\ 2\}) \right\} \\
&= \{LF_{TSfBC,1}, LF_{TSfBC,2}\}.
\end{aligned}$$

Details of the narrated two logical facts are provided in Table 1.

Table 1. Details of the narrated logical facts

Narrated Logical Facts
$LF_{TSfBC,1}$: pixels included in negative areas of $\tilde{t}_{TSfBC,1}$ are most probably true tumour negatives
$LF_{TSfBC,2}$: pixels included in positive areas of $\tilde{t}_{TSfBC,2}$ are most probably true tumour positives

(2) Logical consistency estimation

On the basis of the prediction of the image semantic segmentation model for tumour segmentation for breast cancer (t_{TSfBC}) in section 5.2.2 and the two narrated logical facts $LF_{TSfBC} = \{LF_{TSfBC,1}, LF_{TSfBC,2}\}$, we introduce two reasonings (Reasoning 3 and Reasoning 4). The validity of the two derived reasonings are respectively proved by Proof-R3 and Proof-R4 which are provided in Supplementary.

Reasoning 3. If t_{TSfBC} is given and $LF_{TSfBC,1}$ is given, then the intersection of pixels of t_{TSfBC} that are predicted as tumour positives (t_{TSfBC}^p) and pixels included in negative areas of $\tilde{t}_{TSfBC,1}$ ($\tilde{t}_{TSfBC,1}^n$) can be considered as logically false positives.

Reasoning 4. If t_{TSfBC} is given and $LF_{TSfBC,2}$ is given, then the intersection of pixels of t_{TSfBC} that are predicted as tumour positives (t_{TSfBC}^p) and pixels included in positive areas of $\tilde{t}_{TSfBC,2}$ ($\tilde{t}_{TSfBC,2}^p$) can be considered as logically true positives, and the intersection of pixels of t_{TSfBC} that are predicted as tumour negatives (t_{TSfBC}^n) and pixels included in positive areas of $\tilde{t}_{TSfBC,2}$ ($\tilde{t}_{TSfBC,2}^p$) can be considered as logically false negatives.

Referring to Eq. (6) and using Reasoning 3-4 as p_{TSfBC}^{LCE} , we implement the *LogicalConsistencyEstimate*, which estimates three logical consistencies between t_{TSfBC} and LF_{TSfBC} , as follows

$$\begin{aligned}
LC_{TSfBC} &= LogicalConsistencyEstimate\left(t_{TSfBC}, LF_{TSfBC}; \left\{ \begin{array}{l} Reasoning\ 3, \\ Reasoning\ 4 \end{array} \right\}\right) \\
&= \left\{ LogicalConsistencyEstimate(t_{TSfBC}, LF_{TSfBC,1}; \{Reasoning\ 3\}), \right. \\
&\quad \left. LogicalConsistencyEstimate(t_{TSfBC}, LF_{TSfBC,2}; \{Reasoning\ 4\}) \right\} \\
&= \{LC_{TSfBC,1}, LC_{TSfBC,2}, LC_{TSfBC,3}\}
\end{aligned}$$

Details of the estimated three logical consistencies are provided in Table 2.

Table 2. Details of the estimated logical consistencies

Estimated Logical Consistencies
$LC_{TSfBC,1}$: the intersection of t_{TSfBC}^p and $\tilde{t}_{TSfBC,1}^n$ can be considered as logically false positives
$LC_{TSfBC,2}$: the intersection of t_{TSfBC}^p and $\tilde{t}_{TSfBC,2}^p$ can be considered as logically true positives
$LC_{TSfBC,3}$: the intersection of t_{TSfBC}^n and $\tilde{t}_{TSfBC,2}^p$ can be considered as logically false negatives

(3) Logical assessment metric build

Based on the estimated LC_{TSfBC} , referring to Eq. (6) and using usual definitions for assessment of image semantic segmentation as p_{TSfBC}^{LAM} , we implement *LogicalAssessmentMetricBuild* to abstractly formalize a series of logical assessment metrics, which can be expressed as

$$\begin{aligned}
 LAM_{TSfBC} &= \text{LogicalAssessmentMetricBuild} \left(LC_{TSfBC}; \left\{ \begin{array}{l} TP, FP, FN, \\ precision, recall, \\ f1, fIoU \end{array} \right\} \right) \\
 &= \left\{ LAM_{TSfBC,1}, LAM_{TSfBC,2}, LAM_{TSfBC,3}, \right. \\
 &\quad \left. LAM_{TSfBC,4}, LAM_{TSfBC,5}, LAM_{TSfBC,6}, LAM_{TSfBC,7} \right\}.
 \end{aligned}$$

Details of the built logical assessment metrics are provided in Table 3.

Table 3. Details of the build logical assessment metrics

Built Logical Assessment Metrics
$LAM_{TSfBC,1}$: $LTP = t_{TSfBC}^p \cap \tilde{t}_{TSfBC,2}^p$
$LAM_{TSfBC,2}$: $LFP = t_{TSfBC}^p \cap \tilde{t}_{TSfBC,1}^n$
$LAM_{TSfBC,3}$: $LFN = t_{TSfBC}^n \cap \tilde{t}_{TSfBC,2}^p$
$LAM_{TSfBC,4}$: $Lprecision = \frac{LTP}{LTP+LFP}$
$LAM_{TSfBC,5}$: $Lrecall = \frac{LTP}{LTP+LFN}$
$LAM_{TSfBC,6}$: $Lf1 = \frac{2 \times Lprecision \times Lrecall}{Lprecision + Lrecall}$
$LAM_{TSfBC,7}$: $LfIoU = \frac{LTP}{LTP+LFP+LFN}$

(4) Result

Based on the implemented task specific LAF (LAF_{TSfBC}), we can get a series of abstractly formalized metrics that are suitable for evaluations with IAGTL on TSfBC. As a result, referring to Eq. (6), the abstractly formalized metrics can be denoted by

$$\begin{aligned}
 LAM_{TSfBC} &= LAF: PC(t_{TSfBC}, \tilde{t}_{TSfBC}; \{p_{TSfBC}^{LFN}, p_{TSfBC}^{LCE}, p_{TSfBC}^{LAM}\}) \\
 &= \{LAM_{TSfBC,1}, \dots, LAM_{TSfBC,7}\}.
 \end{aligned}$$

3.3.2 Implementation of method-specific LAF

Regarding to various methods of learning from noisy labels referred in section 5.2.3, we can designate t_{TSfBC} to be associated with a specific method of learning from noisy

labels. With the t_{TSfBC} designated to be associated with a specific method of learning from noisy labels, we can transform the abstractly formalized LAM_{TSfBC} into quantitative values of assessment to implement the method-specific LAF for evaluations with IAGTL on TSfBC. Referring to Eq. (7) and letting ms be a specific method of learning from noisy labels, the transformed quantitative values of assessment can be denoted by

$$\begin{aligned} LAM_{TSfBC,ms} &= LAF:PC(t_{TSfBC,ms}, \tilde{t}_{TSfBC}) \\ &= \{LAM_{TSfBC,ms,1}, \dots, LAM_{TSfBC,ms,7}\}, ms \in \{BaseLine, Forward, \dots, OSAMTL\}. \end{aligned}$$

3.3.3 Implementation of LAF based method performance evaluation

Based on the transformed quantitative values of assessment for evaluations with IAGTL on TSfBC ($LAM_{TSfBC,ms}$), and referring to Eq. (8), we can derive LAF based method performance evaluation (LAF-MPE). For a simple implementation of LAF-MPE, we set the hyper-parameters p^{LMPE} for implementation of *LogicalMethodPerfEval* by ‘selecting the metric of overall performance (SMOP)’, which can be expressed as

$$\begin{aligned} LMP_{TSfBC,ms} &= LogicalMethodPerfEval(LAM_{TSfBC,ms}; 'SMOP') \\ &= \{LAM_{TSfBC,ms,6}, LAM_{TSfBC,ms,7}\}. \end{aligned}$$

4. Verification for Practicability of LAF

On the basis of the application of LAF to two tasks of tumour segmentation for breast cancer (TSfBC) in medical histopathology whole slide image analysis (MHWSIA) presented in Section 3, in this section, we conduct experiments and give corresponding analysis to further verify the practicability of LAF for evaluations with inaccurate ground-truth labels (IAGTLs).

4.1. Preliminary

4.1.1 Overall design

Referring to the summarized practicability of LAF, we consider two key points that need to be experimentally verified to better realize the pros and cons of LAF. The two key points include: 1) on a more difficult task, LAF is able to act like usual strategies for evaluations with AGTLs reasonably; and 2) on an easier task, LAF is unable to act like usual strategies for evaluations with AGTLs confidently.

To verify these two key points, we first conduct experiments that employ LAF to produce evaluations of various methods for learning from inaccurate labels with IAGTLs and experiments that employ usual strategy (US) to produce evaluations of various methods for learning from inaccurate labels with AGTLs, on the two tasks of tumour segmentation for breast cancer (Fig. 2). For each of the two tasks, we conduct two series of experiments including a number of state-of-the-art methods [11–18] for learning from inaccurate labels and their respective combination with an improved version of OSAMTL [7]. As the previous work [7] has confirmed the advantages of the improved OSAMTL series compared with the state-of-the-art series [11–18] using US-based evaluations with AGTLs, we can compare the results of the improved OSAMTL

series with the results of the state-of-the-art series using LAF-based evaluations with IAGTLs to observe whether the LAF-based evaluations with IAGTLs can maintain the advantages of the improved OSAMTL series .

According to the two key points that need to be verified, specifically, we have two expectations in advance: 1) evaluations of LAF with IAGTLs can show the advantages of the improved OSAMTL series compared with the state-of-the-art series, just being able to reasonably act like evaluations of US with AGTLs on the task of tumour segmentation in HE-stained post-treatment surgical resection images which is more difficult; 2) evaluations of LAF with IAGTLs cannot show the advantages of the improved OSAMTL series compared with the state-of-the-art series, just being unable to confidently act like evaluations of US with AGTLs on the task of tumour segmentation in HE-stained pre-treatment biopsy images which is easier.

4.1.2 Data preparation

For evaluations with IAGTLs using LAF on the task of tumour segmentation in HE-stained pre-treatment biopsy images, we prepared 248 image patches with IAGTLs (1) corresponding to $\tilde{t}_{TSfBC,1}$ and 36 image patches with IAGTLs (2) corresponding to $\tilde{t}_{TSfBC,2}$. For evaluations with AGTLs using US on the task of tumour segmentation in HE-stained pre-treatment biopsy images, we prepared 158 image patches with corresponding AGTLs.

For evaluations with IAGTLs using LAF on the task of tumour segmentation in HE-stained post-treatment surgical resection images, we prepared 736 image patches with IAGTLs (1) corresponding to $\tilde{t}_{TSfBC,1}$ and 358 image patches with IAGTLs (2) corresponding to $\tilde{t}_{TSfBC,2}$. For evaluations with AGTLs using US on the task of tumour segmentation in HE-stained pre-treatment biopsy images, we prepared 242 image patches with corresponding AGTLs.

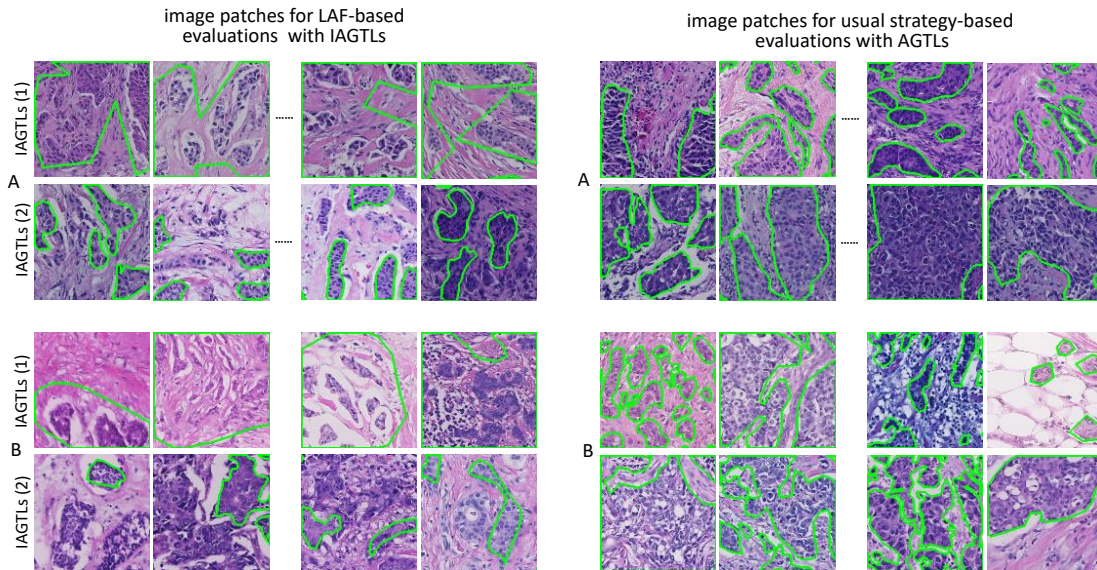


Figure. 3. Examples of the image patches prepared for evaluations with IAGTLs or AGTLs on the two tasks of TSfBC. A: the task of tumour segmentation in HE-stained pre-treatment biopsy images. B: the task of tumour segmentation in HE-stained post-treatment surgical resection images.

The image patches prepared for experiments were cropped at 10× magnification of some digital whole slide images and the size of each cropped image patch was at 256 × 256 pixels (width × height). Some examples of the image patches prepared for evaluations with IAGTLs or AGTLs on the two tasks are provided as Fig. 3. From Fig. 3, we can note that the preparation of the image patches for evaluations with IAGTLs are much less labour extensive than the preparation of the image patches for evaluations with AGTLs.

4.1.3 Experimental settings

All of our experiments were performed on an Intel core Xeon E5–2630 v4s with a memory capacity of 128GB and eight NVIDIA GTX 1080Ti GPUs. Our developing environment is based on Tensorflow 1.10.1 and Python 3.5. More detailed experimental settings for training the image semantic segmentation model with the two series of methods of learning from inaccurate labels to produce the predictions can be found in our previous work [7].

4.2. Results of LAF-based evaluations with IAGTLs

Referring to the implementations of LAF applied on TSfBC presented in Section 3, the LAM and LMP results of LAF-based evaluations with IAGTLs for various methods of learning from inaccurate labels for the tumour segmentation in HE-stained pre-treatment biopsy images and the tumour segmentation in HE-stained post-treatment surgical resection images are respective shown as Table 4 and Table 5.

Table 4. LAF-based evaluations with IAGTLs on the task of tumour segmentation in HE-stained pre-treatment biopsy images

Solution	LAM						LMP	
	LTP	LFP	LFN	Lprecision	Lrecall	Lf1	LfloU	
BaseLine	17619	6956	1698	71.69	91.21	80.28	67.06	
Forward	17455	5680	1861	75.45	90.37	82.24	69.83	
Backward	15175	7032	4141	68.33	78.56	73.09	57.59	
Boost-Hard	17497	7104	1820	71.12	90.58	79.68	66.22	
Boost-Soft	15685	6564	3631	70.50	81.20	75.47	60.61	
D2I	17506	7697	1811	69.46	90.62	78.64	64.80	
SCE	16627	5601	2690	74.80	86.07	80.04	66.73	
Peer	17669	6775	1648	72.28	91.47	80.75	67.72	
DT-Forward	16731	5814	2586	74.21	86.61	79.93	66.58	
NCE-SCE	16901	6605	2415	71.90	87.50	78.94	65.20	
BaseLine_OSAMTL	15428	4165	3888	78.74	79.87	79.30	65.70	
Forward_OSAMTL	14132	3282	5184	81.15	73.16	76.95	62.54	
Backward_OSAMTL	15414	3816	3902	80.16	79.8	79.98	66.63	
Boost-Hard_OSAMTL	14928	3812	4389	79.66	77.28	78.45	64.54	
Boost-Soft_OSAMTL	15511	5198	3805	74.9	80.3	77.51	63.27	
D2I_OSAMTL	15220	4267	4097	78.1	78.79	78.45	64.54	
SCE_OSAMTL	14982	4264	4334	77.84	77.56	77.7	63.54	
Peer_OSAMTL	14637	4182	4680	77.78	75.77	76.76	62.29	
DT-Forward_OSAMTL	14675	2956	4641	83.23	75.97	79.44	65.89	
NCE-SCE_OSAMTL	14238	3993	5078	78.1	73.71	75.84	61.08	

Table 5. LAF-based evaluations with IAGTLs on the task of tumour segmentation in HE-stained post-treatment surgical resection images

Solution	LAM						
	LTP	LFP	LFN	Lprecision	Lrecall	LMP	
						Lfl	LfIoU
BaseLine	16131	7863	4525	67.23	78.09	72.26	56.56
Forward	14933	7440	5723	66.75	72.29	69.41	53.15
Backward	15196	8983	5460	62.85	73.57	67.79	51.27
Boost-Hard	15829	8878	4826	64.07	76.64	69.79	53.60
Boost-Soft	17123	9318	3533	64.76	82.90	72.71	57.13
D2I	16039	9634	4617	62.47	77.65	69.24	52.95
SCE	15099	7907	5567	65.63	73.06	69.15	52.84
Peer	15896	10532	4759	60.15	76.96	67.52	50.97
DT-Forward	13787	5248	6869	72.43	66.75	69.47	53.22
NCE-SCE	14319	7150	6337	66.70	69.32	67.98	51.50
BaseLine_OSAMTL	16163	2230	4492	87.88	78.25	82.79	70.63
Forward_OSAMTL	16197	2860	4459	84.99	78.41	81.57	68.88
Backward_OSAMTL	16167	3331	4489	82.92	78.27	80.52	67.4
Boost-Hard_OSAMTL	16560	2589	4095	86.48	80.17	83.21	71.24
Boost-Soft_OSAMTL	15778	2917	4878	84.4	76.38	80.19	66.93
D2I_OSAMTL	16108	2074	4547	88.59	77.99	82.95	70.87
SCE_OSAMTL	14907	2961	5748	83.43	72.17	77.39	63.12
Peer_OSAMTL	16983	4091	3673	80.59	82.22	81.39	68.63
DT-Forward_OSAMTL	15927	2045	4729	88.62	77.11	82.46	70.16
NCE-SCE_OSAMTL	15540	1971	5116	88.74	75.23	81.43	68.68

4.3. Results of US-based evaluations with AGTLs

The results of US-based evaluations with AGTLs for various methods of learning from inaccurate labels for the tumour segmentation in HE-stained pre-treatment biopsy images and the tumour segmentation in HE-stained post-treatment surgical resection images are respective shown as Table 6 and Table 7.

Table 6. US-based evaluations with AGTLs on the task of tumour segmentation in HE-stained pre-treatment biopsy images

Solution	TP	FP	FN	precision	recall	f1	fIoU
BaseLine	22707	13298	3249	63.07	87.48	73.29	57.85
Forward	23494	15160	2462	60.78	90.51	72.73	57.14
Backward	21858	13453	4098	61.90	84.21	71.35	55.46
Boost-Hard	22184	12652	3771	63.68	85.47	72.98	57.46
Boost-Soft	23724	15849	2231	59.95	91.40	72.41	56.75
D2I	23068	14632	2888	61.19	88.87	72.48	56.83
SCE	22753	13499	3203	62.76	87.66	73.15	57.67
Peer	22658	12704	3298	64.07	87.29	73.90	58.61
DT-Forward	23280	14239	2676	62.05	89.69	73.35	57.92
NCE-SCE	23395	14452	2561	61.81	90.13	73.34	57.90
BaseLine_OSAMTL	21010	6381	4946	76.70	80.94	78.77	64.97
Forward_OSAMTL	20215	5579	5740	78.37	77.88	78.13	64.11
Backward_OSAMTL	20818	6124	5137	77.27	80.21	78.71	64.9
Boost-Hard_OSAMTL	20230	5732	5725	77.92	77.94	77.93	63.84
Boost-Soft_OSAMTL	20657	5936	5298	77.68	79.59	78.62	64.77
D2I_OSAMTL	20348	5981	5608	77.28	78.39	77.83	63.71

SCE_OSAMTL	19719	5651	6236	77.73	75.97	76.84	62.39
Peer_OSAMTL	20379	6634	5577	75.44	78.51	76.95	62.53
DT-Forward_OSAMTL	19958	5347	5998	78.87	76.89	77.87	63.76
NCE-SCE_OSAMTL	18712	4594	7244	80.29	72.09	75.97	61.25

Table 7. US-based evaluations with AGTLs on the task of tumour segmentation in HE-stained post-treatment surgical resection images

Solution	TP	FP	FN	precision	recall	f1	fIoU
BaseLine	15446	13831	8467	52.76	64.59	58.08	40.92
Forward	15129	13409	8783	53.01	63.27	57.69	40.54
Backward	16373	17083	7540	48.94	68.47	57.08	39.94
Boost-Hard	16599	15904	7313	51.07	69.42	58.85	41.69
Boost-Soft	19000	18353	4912	50.87	79.46	62.03	44.95
D2I	16331	14876	7581	52.33	68.30	59.26	42.10
SCE	15604	13286	8309	54.01	65.25	59.10	41.95
Peer	17366	19348	6546	47.30	72.62	57.29	40.14
DT-Forward	15374	15525	8538	49.76	64.29	56.10	38.98
NCE-SCE	16356	16574	7556	49.67	68.40	57.55	40.40
BaseLine_OSAMTL	16000	5649	7912	73.91	66.91	70.24	54.13
Forward_OSAMTL	14825	3948	9088	78.97	62.00	69.46	53.21
Backward_OSAMTL	15441	5648	8471	73.22	65.57	68.62	52.24
Boost-Hard_OSAMTL	15713	4611	8200	77.31	65.71	71.04	55.09
Boost-Soft_OSAMTL	15799	6017	8114	72.42	66.07	69.10	52.79
D2I_OSAMTL	15109	3599	8803	80.76	63.18	70.90	54.92
SCE_OSAMTL	15168	5151	8744	74.65	63.43	68.59	52.19
Peer_OSAMTL	16954	7478	6958	69.39	70.90	70.14	54.01
DT-Forward_OSAMTL	15175	4483	8737	77.20	63.46	69.66	53.44
NCE-SCE_OSAMTL	13101	2749	10811	82.66	54.79	65.90	49.14

4.4. Comparison between LAF and US

For the comparison between LAF and US, we compute the mean values with corresponding confident intervals (CI) and the P values of the overall performances for the state-of-the-art methods (SotA) and SotA combined with the improved OSAMTL (SotA-OSAMTL). The results for LAF-based evaluations with IAGTLs (Lf1 and LfIoU) and US-based evaluations with AGTLs (f1 and fIoU) on the task of tumour segmentation in HE-stained pre-treatment biopsy images (i.e., easier task) are shown as Table 8. The results for LAF-based evaluations with IAGTLs (Lf1 and LfIoU) and US-based evaluations with AGTLs (f1 and fIoU) on the task of tumour segmentation in HE-stained post-treatment surgical resection images (i.e., more difficult task) are shown as Table 9.

Table 8. Results for LAF-based evaluations (Lf1 and LfIoU) and US-based evaluations (f1 and fIoU) on easier task.

Solution(Metric)	SotA(Lf1)	SotA(LfIoU)	SotA(f1)	SotA(fIoU)
Mean(CI)	78.91(76.36-81.46)	65.23(61.83-68.63)	72.90(72.23-73.57)	57.36(56.53-58.19)
SotA-OSAMTL(Lf1)				
78.04(76.78-79.29)	P=0.372			
SotA-OSAMTL(LfIoU)				
64.00(62.32-65.68)		P=0.343		
SotA-OSAMTL(f1)			P<0.001	

77.76(76.89-78.63)

SotA-OSAMTL(fIoU)

63.62(62.46-64.78)

P<0.001

Table 9. Results for LAF-based evaluations (Lf1 and LfIoU) and US-based evaluations (f1 and fIoU) on more difficult task.

Solution(Metric) Mean(CI)	SotA(Lf1) 69.53(67.88-71.19)	SotA(LfIoU) 53.32(51.36-55.28)	SotA(f1) 58.30(56.75-59.86)	SotA(fIoU) 41.16(39.60-42.72)
SotA-OSAMTL(Lf1) 81.39(79.74-83.04)	P<0.001			
SotA-OSAMTL(LfIoU) 68.65(66.35-70.96)		P<0.001		
SotA-OSAMTL(f1) 69.37(67.96-70.77)			P<0.001	
SotA-OSAMTL(fIoU) 53.12(51.48-54.75)				P<0.001

4.5. Analysis

From Table 8, we can summarize that, on the easier task, the results of US-based evaluations with AGTLs (f1 and fIoU) show the advantages of the SotA-OSAMTL series compared with the SotA series (f1: P<0.001, fIoU: P<0.001) while the results of LAF-based evaluations with IAGTLs (Lf1 and LfIoU) do not show the same conclusions (Lf1: P=0.372, LfIoU: P=0.343). Since the previous work [7] has confirmed the advantages of the improved OSAMTL series compared with the state-of-the-art series [11–18] using US-based evaluations with AGTLs, the summarization from Table 8 indicates that evaluations of LAF with IAGTLs cannot show the advantages of the SotA-OSAMTL series compared with the StoA series, just being unable to confidently act like evaluations of US with AGTLs on the easier task.

From Table 9, we can summarize that, on the more difficult task, the results of US-based evaluations with AGTLs (f1 and fIoU) show the advantages of the SotA-OSAMTL series compared with the SotA series (f1: P<0.001, fIoU: P<0.001) while the results of LAF-based evaluations with IAGTLs (Lf1 and LfIoU) as well show the same conclusions (Lf1: P<0.001, LfIoU: P<0.001). Identically, since the previous work [7] has confirmed the advantages of the improved OSAMTL series compared with the state-of-the-art series [11–18] using US-based evaluations with AGTLs, the summarization from Table 9 indicates that evaluations of LAF with IAGTLs can show the advantages of the SotA-OSAMTL series compared with the StoA series, just being able to reasonably act like evaluations of US with AGTLs on the more difficult task.

As a result, the summarizations from Table 8 and 9 reflect that the practicability of LAF for evaluations with IAGTLs is valid with the case of TSfBC in MHWSIA.

5. Conclusion and Discussion

In this paper, we validate the practicability of logical assessment formula (LAF) for evaluations with inaccurate ground-truth labels (IAGTLs). The practicability of LAF for evaluations with IAGTLs include: 1) LAF can be applied for evaluations with IAGTLs on a more difficult task, able to act like usual strategies for evaluations with

AGTLs reasonably; and 2) LAF can be applied for evaluations with IAGTLs simply from the logical point of view on an easier task, unable to act like usual strategies for evaluations with AGTLs confidently. We applied LAF to two tasks of tumour segmentation for breast cancer (TSfBC) in medical histopathology whole slide image analysis (MHWSIA), and implemented a specific LAF solution that is suitable for evaluations with IAGTLs in the case of TSfBC in MHWSIA. Experimental results and analyses of this application support that the practicability of LAF for evaluations with IAGTLs is valid with the case of TSfBC in MHWSIA. Thus, the primary significance of this paper is that it reports the first positive case that reflects the potentials of LAF applied to MHWSIA for evaluations with IAGTLs.

Although the application of LAF to TSfBC in MHWSIA showed good support for the practicability of LAF, the problem remains unsolved is how to estimate that a given task is a difficult one or an easy one in the application of LAF for evaluations without AGTL. Since the practicability of LAF reflects that evaluations of LAF with IAGTLs on a difficult task are more reliable (more consistent with evaluations of usual strategies with AGTL) than on an easier task, the definition of a given task to be difficult or easy is the key foundation for the application of LAF for evaluations with IAGTL. In this paper, the estimation of the two tasks of TSfBC in MHWSIA to be difficult or easy is qualitatively formed by the problem analyses and suggestions from pathology experts [7] (section 3.1), and fortunately the two tasks are suitable to validate the practicability of LAF. This specific validation demonstrates the practicability of LAF is valid with the case of TSfBC in MHWSIA, but it is not persuasive enough to help deciding whether LAF is suitable for evaluations IAGTL on any other given task. However, if the difficulty of a given task can be quantitatively estimated, then it will be much easy for us to decide whether LAF is suitable for evaluations with IAGTL on the given task via an appropriate threshold of task difficulty. Moreover, more applications of LAF applied to other tasks need to be conducted. In future works, these issues should be addressed.

Acknowledgments

We acknowledge Dr. Yani Wei and Dr. Fengling Li for providing the annotations for the data used for experiments when they were PhD candidates supervised by Professor Hong Bu. Their contributions were also more detailly acknowledged in previous works [7,19,20].

Reference

- [1] Y. Yang, Logical Assessment Formula and Its Principles for Evaluations with Inaccurate Ground-Truth Labels, (2021). <http://arxiv.org/abs/2110.11567>.
- [2] H.H. Chang, A.H. Zhuang, D.J. Valentino, W.C. Chu, Performance measure characterization for evaluating neuroimage segmentation algorithms, Neuroimage. (2009). <https://doi.org/10.1016/j.neuroimage.2009.03.068>.
- [3] A.A. Taha, A. Hanbury, Metrics for evaluating 3D medical image segmentation: analysis, selection, and tool, BMC Med. Imaging. 15 (2015) 29. <https://doi.org/10.1186/s12880-015-0068-x>.

- [4] H. M, S. M.N, A Review on Evaluation Metrics for Data Classification Evaluations, *Int. J. Data Min. Knowl. Manag. Process.* 5 (2015) 01–11. <https://doi.org/10.5121/ijdkp.2015.5201>.
- [5] H.J. Jung, M. Lease, Evaluating Classifiers Without Expert Labels, (2012). <https://doi.org/10.48550/arxiv.1212.0960>.
- [6] W. Deng, L. Zheng, Are Labels Always Necessary for Classifier Accuracy Evaluation?, (2021) 15069–15078. https://openaccess.thecvf.com/content/CVPR2021/html/Deng_Are_Labels_Always_Necessary_for_Classifier_Accuracy_Evaluation_CVPR_2021_paper.html (accessed April 19, 2022).
- [7] Y. Yang, F. Li, Y. Wei, J. Chen, N. Chen, H. Bu, One-Step Abductive Multi-Target Learning with Diverse Noisy Samples and Its Application to Tumour Segmentation for Breast Cancer, (2021). <http://arxiv.org/abs/2110.10325> (accessed January 20, 2022).
- [8] B. Frénay, M. Verleysen, Classification in the presence of label noise: A survey, *IEEE Trans. Neural Networks Learn. Syst.* (2014). <https://doi.org/10.1109/TNNLS.2013.2292894>.
- [9] H. Song, M. Kim, D. Park, Y. Shin, J.-G. Lee, Learning from Noisy Labels with Deep Neural Networks: A Survey, (2020). <http://arxiv.org/abs/2007.08199> (accessed August 12, 2020).
- [10] Y. Yang, Y. Yang, J. Chen, J. Zheng, Z. Zheng, Handling Noisy Labels via One-Step Abductive Multi-Target Learning: An Application to Helicobacter Pylori Segmentation, (2020). <http://arxiv.org/abs/2011.14956>.
- [11] G. Patrini, A. Rozza, A.K. Menon, R. Nock, L. Qu, Making deep neural networks robust to label noise: A loss correction approach, in: *Proc. - 30th IEEE Conf. Comput. Vis. Pattern Recognition, CVPR 2017, 2017*. <https://doi.org/10.1109/CVPR.2017.240>.
- [12] S.E. Reed, H. Lee, D. Anguelov, C. Szegedy, D. Erhan, A. Rabinovich, Training deep neural networks on noisy labels with bootstrapping, in: *3rd Int. Conf. Learn. Represent. ICLR 2015 - Work. Track Proc., 2015*.
- [13] E. Arazo, D. Ortego, P. Albert, N.E. O’Connor, K. McGuinness, Unsupervised label noise modeling and loss correction, in: *36th Int. Conf. Mach. Learn. ICML 2019, 2019*.
- [14] X. Ma, Y. Wang, M.E. Houle, S. Zhou, S.M. Erfani, S.T. Xia, S. Wijewickrema, J. Bailey, Dimensionality-Driven learning with noisy labels, in: *35th Int. Conf. Mach. Learn. ICML 2018, 2018*.
- [15] Y. Wang, X. Ma, Z. Chen, Y. Luo, J. Yi, J. Bailey, Symmetric cross entropy for robust learning with noisy labels, in: *Proc. IEEE Int. Conf. Comput. Vis., 2019*. <https://doi.org/10.1109/ICCV.2019.00041>.
- [16] Y. Liu, H. Guo, Peer loss functions: Learning from noisy labels without knowing noise rates, in: *37th Int. Conf. Mach. Learn. ICML 2020, 2020*.
- [17] Y. Yao, T. Liu, B. Han, M. Gong, J. Deng, G. Niu, M. Sugiyama, Dual T: Reducing estimation error for transition matrix in label-noise learning, in: *Adv. Neural Inf. Process. Syst., 2020*.
- [18] X. Ma, H. Huang, Y. Wang, S.R.S. Erfani, J. Bailey, Normalized loss functions for deep learning with noisy labels, in: *37th Int. Conf. Mach. Learn. ICML 2020, 2020*.
- [19] Y. Yang, J. Chen, Y. Wei, M. Alobaidi, H. Bu, Experts’ cognition-driven safe noisy labels learning for precise segmentation of residual tumor in breast cancer, (2023). <http://arxiv.org/abs/2304.07295>.

- [20] Y. Yang, F. Li, Y. Wei, Y. Zhao, J. Fu, X. Xiao, H. Bu, Experts' cognition-driven ensemble deep learning for external validation of predicting pathological complete response to neoadjuvant chemotherapy from histological images in breast cancer, (2023). <http://arxiv.org/abs/2306.10805>.

Supplementary

Preliminary of Logical Reasoning

We introduce some propositional connectives and rules for proof of propositional logical reasoning, which are respectively shown as Table 1 and Table 2, for the logical reasonings conducted in this paper.

Table 1. Propositional connectives

Connective	Meaning
\wedge	conjunction
\rightarrow	implication

Table 2. Rules for proof of propositional logical reasoning, \vdash denotes 'bring out'

Rule	Meaning
$\wedge -$	reductive law of conjunction: $A \wedge B, \vdash A$ or B .
$\wedge +$	additional law of conjunction: $A, B, \vdash A \wedge B$.
MP	modus ponens: $A \rightarrow B, A, \vdash B$.
HS	hypothetical syllogism: $A \rightarrow B, B \rightarrow C, \vdash A \rightarrow C$.

Proof of Reasoning 1

Reasoning 1. *If $\tilde{t}_{TSfBC,1}$ is given, then pixels included in negative areas of $\tilde{t}_{TSfBC,1}$ are most probably true tumour negatives.*

Proof-R1. Firstly, with the given $\tilde{t}_{TSfBC,1}$, we have following preconditions for Reasoning 1.

1. If $\tilde{t}_{TSfBC,1}$ is given, then the recall of positive areas of $\tilde{t}_{TSfBC,1}$ to represent true tumour positives is very high.
2. If the recall of positive areas of $\tilde{t}_{TSfBC,1}$ to represent true tumour positives is very high, then almost all of true tumour positives are included in positive areas of $\tilde{t}_{TSfBC,1}$.
3. If almost all of true tumour positives are included in positive areas of $\tilde{t}_{TSfBC,1}$, then true tumour positives included in negative areas of $\tilde{t}_{TSfBC,1}$ are rare.
4. If true tumour positives included in negative areas of $\tilde{t}_{TSfBC,1}$ are rare, then pixels included in negative areas of $\tilde{t}_{TSfBC,1}$ are mostly probably true tumour negatives.

Secondly, we give the propositional symbols for the above preconditions 1-4 for Reasoning 1, which are shown in Table 3.

Table 3. Propositional symbols of preconditions for Reasoning 1

Symbol	Meaning
<i>a</i>	$\tilde{t}_{TSfBC,1}$ is given
<i>b</i>	the recall of positive areas of $\tilde{t}_{TSfBC,1}$ to represent true tumour positives is very high
<i>c</i>	almost all of true tumour positives are included in positive areas of $\tilde{t}_{TSfBC,1}$
<i>d</i>	true tumour positives included in negative areas of $\tilde{t}_{TSfBC,1}$ are rare
<i>e</i>	pixels included in negative areas of $\tilde{t}_{TSfBC,1}$ are mostly probably true tumour negatives

Thirdly, referring to Table 3, we signify the propositional formalizations of the preconditions 1-4 for Reasoning 1 and Reasoning 1 via the propositional connectives listed in Table 1 as follows.

- | | |
|----------------------|--------------|
| 1) $a \rightarrow b$ | Precondition |
| 2) $b \rightarrow c$ | Precondition |
| 3) $c \rightarrow d$ | Precondition |
| 4) $d \rightarrow e$ | Precondition |
| $a \rightarrow e$ | Reasoning 1 |

Fourthly, we show the validity of Reasoning 1 via the rules for proof of propositional logical reasoning listed in Table 2 as follows.

$\therefore a \rightarrow e$

- | | |
|-----------------------|--------------------------|
| 5) a | Hypothesis |
| 6) $a \rightarrow c$ | 1),2); HS |
| 7) $c \rightarrow e$ | 3),4); HS |
| 8) $a \rightarrow e$ | 6),7); HS |
| 9) e | 8),5); MP |
| 10) $a \rightarrow e$ | 5)-9); Conditional Proof |

Since the hypothesis a of the 5) step has been fulfilled by the abduced $\tilde{t}_{TSfBC} = \{\tilde{t}_{TSfBC,1}, \tilde{t}_{TSfBC,2}\}$ in section 5.2.2, Reasoning 1 is proved to be valid.

Proof of Reasoning 2

Reasoning 2. If $\tilde{t}_{TSfBC,2}$ is given, then pixels included in positive areas of $\tilde{t}_{TSfBC,2}$ are most probably true tumour positives.

Proof-R2. Firstly, with the given $\tilde{t}_{TSfBC,2}$, we have following preconditions for Reasoning 2.

1. If $\tilde{t}_{TSfBC,2}$ is given, then the precision of positive areas of $\tilde{t}_{TSfBC,2}$ to represent true tumour positives is very high.
2. If the precision of positive areas of $\tilde{t}_{TSfBC,2}$ to represent true tumour positives is very high, then the positive areas of $\tilde{t}_{TSfBC,2}$ are almost all true tumour positives.
3. If the positive areas of $\tilde{t}_{TSfBC,2}$ are almost all true tumour positives, then false tumour positives included in positive areas of $\tilde{t}_{TSfBC,2}$ are rare.
4. If false tumour positives included in positive areas of $\tilde{t}_{TSfBC,2}$ are rare, then pixels included in positive areas of $\tilde{t}_{TSfBC,2}$ are most probably true tumour positives.

Secondly, we give the propositional symbols for the above preconditions 1-4 for Reasoning 2, which are shown in Table 4.

Table 4. Propositional symbols of preconditions for Reasoning 2

Symbol	Meaning
f	$\tilde{t}_{TSfBC,2}$ is given
g	the precision of positive areas of $\tilde{t}_{TSfBC,2}$ to represent true tumour positives is very high
h	the positive areas of $\tilde{t}_{TSfBC,2}$ are almost all true tumour positives
i	false tumour positives included in positive areas of $\tilde{t}_{TSfBC,2}$ are rare
j	pixels included in positive areas of $\tilde{t}_{TSfBC,2}$ are most probably true tumour positives

Thirdly, referring to Table 4, we signify the propositional formalizations of the preconditions 1-4 for Reasoning 2 and Reasoning 2 via the propositional connectives listed in Table 1 as follows.

- | | |
|----------------------|--------------|
| 1) $f \rightarrow g$ | Precondition |
| 2) $g \rightarrow h$ | Precondition |
| 3) $h \rightarrow i$ | Precondition |
| 4) $i \rightarrow j$ | Precondition |
| $f \rightarrow j$ | Reasoning 2 |

Fourthly, we show the validity of Reasoning 2 via the rules for proof of propositional logical reasoning listed in Table 2 as follows.

$\therefore f \rightarrow j$

5) f	Hypothesis
6) $f \rightarrow h$	1),2); HS
7) $h \rightarrow j$	3),4); HS
8) $f \rightarrow j$	6),7); HS
9) j	8),5); MP
10) $f \rightarrow j$	5)-9); Conditional Proof

Since the hypothesis f of the 5) step has been fulfilled by the abduced $\tilde{t}_{TSfBC} = \{\tilde{t}_{TSfBC,1}, \tilde{t}_{TSfBC,2}\}$ in section 5.2.2, Reasoning 2 is proved to be valid.

Proof of Reasoning 3

Reasoning 3. If t_{TSfBC} is given and $LF_{TSfBC,1}$ is given, then the intersection of pixels of t_{TSfBC} that are predicted as tumour positives (t_{TSfBC}^p) and pixels included in negative areas of $\tilde{t}_{TSfBC,1}$ ($\tilde{t}_{TSfBC,1}^n$) can be considered as logically false positives.

Proof-R3. Firstly, with the given t_{TSfBC} and $LF_{TSfBC,1}$, we have following preconditions for Reasoning 3.

1. If $LF_{TSfBC,1}$ is given, then $\tilde{t}_{TSfBC,1}$ is given.
2. If $\tilde{t}_{TSfBC,1}$ is given, then pixels included in negative areas of $\tilde{t}_{TSfBC,1}$ ($\tilde{t}_{TSfBC,1}^n$) are most probably true tumour negatives. (Reasoning 1)
3. If t_{TSfBC} is given, then pixels of t_{TSfBC} that are predicted as tumour positives (t_{TSfBC}^p) exist.
4. If pixels included in negative areas of $\tilde{t}_{TSfBC,1}$ ($\tilde{t}_{TSfBC,1}^n$) are most probably true tumour negatives and pixels of t_{TSfBC} that are predicted as tumour positives (t_{TSfBC}^p) exist, then the intersection of pixels included in t_{TSfBC}^p and pixels included in $\tilde{t}_{TSfBC,1}^n$ can be considered as most probably predicted false tumour positives.
5. If the intersection of pixels included in t_{TSfBC}^p and pixels included in $\tilde{t}_{TSfBC,1}^n$ can be considered as most probably predicted false tumour positives, then the intersection of pixels included in t_{TSfBC}^p and pixels included in $\tilde{t}_{TSfBC,1}^n$ can be considered as logically false positives.
6. If the intersection of pixels included in t_{TSfBC}^p and pixels included in $\tilde{t}_{TSfBC,1}^n$ can be considered as logically false positives, then the intersection of pixels of t_{TSfBC}

that are predicted as tumour positives (t_{TSfBC}^p) and pixels included in negative areas of $\tilde{t}_{TSfBC,1}$ ($\tilde{t}_{TSfBC,1}^n$) can be considered as logically false positives.

Secondly, we give the propositional symbols for the above preconditions 1-6 for Reasoning 3, which are shown in Table 5.

Table 5. Propositional symbols of preconditions for Reasoning 3

Symbol	Meaning
k	$LF_{TSfBC,1}$ is given
l	$\tilde{t}_{TSfBC,1}$ is given
m	pixels included in negative areas of $\tilde{t}_{TSfBC,1}$ ($\tilde{t}_{TSfBC,1}^n$) are most probably true tumour negatives
n	t_{TSfBC} is given
o	pixels of t_{TSfBC} that are predicted as tumour positives (t_{TSfBC}^p) exist
p	the intersection of pixels included in t_{TSfBC}^p and pixels included in $\tilde{t}_{TSfBC,1}^n$ can be considered as most probably predicted false tumour positives
q	the intersection of pixels included in t_{TSfBC}^p and pixels included in $\tilde{t}_{TSfBC,1}$ can be considered as logically false positives
r	the intersection of pixels of t_{TSfBC} that are predicted as tumour positives (t_{TSfBC}^p) and pixels included in negative areas of $\tilde{t}_{TSfBC,1}$ ($\tilde{t}_{TSfBC,1}^n$) can be considered as logically false positives

Thirdly, referring to Table 5, we signify the propositional formalizations of the preconditions 1-6 for Reasoning 3 and Reasoning 3 via the propositional connectives listed in Table 1 as follows.

- | | |
|---------------------------------|--------------|
| 1) $k \rightarrow l$ | Precondition |
| 2) $l \rightarrow m$ | Precondition |
| 3) $n \rightarrow o$ | Precondition |
| 4) $(m \wedge o) \rightarrow p$ | Precondition |
| 5) $p \rightarrow q$ | Precondition |
| 6) $q \rightarrow r$ | Precondition |
| $(n \wedge k) \rightarrow r$ | Reasoning 3 |

Fourthly, we show the validity of Reasoning 3 via the rules for proof of propositional logical reasoning listed in Table 2 as follows.

$$\therefore (n \wedge k) \rightarrow r$$

7) $n \wedge k$	Hypothesis
8) n	7); $\wedge -$
9) k	7); $\wedge -$
10) l	1),9); MP
11) m	2),10); MP
12) o	3),8); MP
13) $m \wedge o$	11),12); $\wedge +$
14) $(m \wedge o) \rightarrow q$	4),5); HS
15) $(m \wedge o) \rightarrow r$	14),6); HS
16) r	15),13); MP
17) $(n \wedge k) \rightarrow r$	7)-16); Conditional Proof

Since the hypothesis $n \wedge k$ of the 7) step has been fulfilled by the prediction of the image semantic segmentation model for tumour segmentation for breast cancer (t_{TSfBC}) in section 5.2.3 and the two narrated logical facts $LF_{TSfBC} = \{LF_{TSfBC,1}, LF_{TSfBC,2}\}$, Reasoning 3 is proved to be valid.

Proof of Reasoning 4

Reasoning 4. *If t_{TSfBC} is given and $LF_{TSfBC,2}$ is given, then the intersection of pixels of t_{TSfBC} that are predicted as tumour positives (t_{TSfBC}^p) and pixels included in positive areas of $\tilde{t}_{TSfBC,2}$ ($\tilde{t}_{TSfBC,2}^p$) can be considered as logically true positives, and the intersection of pixels of t_{TSfBC} that are predicted as tumour negatives (t_{TSfBC}^n) and pixels included in positive areas of $\tilde{t}_{TSfBC,2}$ ($\tilde{t}_{TSfBC,2}^p$) can be considered as logically false negatives.*

Proof-R4. Firstly, with the given t_{TSfBC} and $LF_{TSfBC,2}$, we have following preconditions for Reasoning 4.

1. If $LF_{TSfBC,2}$ is given, then $\tilde{t}_{TSfBC,2}$ is given.
2. If $\tilde{t}_{TSfBC,2}$ is given, then pixels included in positive areas of $\tilde{t}_{TSfBC,2}$ ($\tilde{t}_{TSfBC,2}^p$) are most probably true tumour positives. (Reasoning 2)
3. If t_{TSfBC} is given, then pixels of t_{TSfBC} that are predicted as tumour positives (t_{TSfBC}^p) exist and pixels of t_{TSfBC} that are predicted as tumour negatives (t_{TSfBC}^n) exist.

4. If pixels included in positive areas of $\tilde{t}_{TSfBC,2}$ ($\tilde{t}_{TSfBC,2}^p$) are most probably true tumour positives and pixels of t_{TSfBC} that are predicted as tumour positives (t_{TSfBC}^p) exist, then the intersection of pixels included in t_{TSfBC}^p and pixels included in $\tilde{t}_{TSfBC,2}^p$ can be considered as most probably predicted true tumour positives.
5. If pixels included in positive areas of $\tilde{t}_{TSfBC,2}$ ($\tilde{t}_{TSfBC,2}^p$) are most probably true tumour positives and pixels of t_{TSfBC} that are predicted as tumour negatives (t_{TSfBC}^n) exist, then the intersection of pixels included in t_{TSfBC}^n and pixels included in $\tilde{t}_{TSfBC,2}^p$ can be considered as most probably predicted false tumour negatives.
6. If the intersection of pixels included in t_{TSfBC}^p and pixels included in $\tilde{t}_{TSfBC,2}^p$ can be considered as most probably predicted true tumour positives, then the intersection of pixels included in t_{TSfBC}^p and pixels included in $\tilde{t}_{TSfBC,2}^p$ can be considered as logically true positives.
7. If the intersection of pixels included in t_{TSfBC}^n and pixels included in $\tilde{t}_{TSfBC,2}^p$ can be considered as most probably predicted false tumour negatives, then the intersection of pixels included in t_{TSfBC}^n and pixels included in $\tilde{t}_{TSfBC,2}^p$ can be considered as logically false negatives.
8. If the intersection of pixels included in t_{TSfBC}^p and pixels included in $\tilde{t}_{TSfBC,2}^p$ can be considered as logically true positives, then the intersection of pixels of t_{TSfBC} that are predicted as tumour positives (t_{TSfBC}^p) and pixels included in positive areas of $\tilde{t}_{TSfBC,2}$ ($\tilde{t}_{TSfBC,2}^p$) can be considered as logically true positives.
9. If the intersection of pixels included in t_{TSfBC}^n and pixels included in $\tilde{t}_{TSfBC,2}^p$ can be considered as logically false negatives, then the intersection of pixels of t_{TSfBC} that are predicted as tumour negatives (t_{TSfBC}^n) and pixels included in positive areas of $\tilde{t}_{TSfBC,2}$ ($\tilde{t}_{TSfBC,2}^p$) can be considered as logically false negatives.

Secondly, we give the propositional symbols for the above preconditions 1-9 for Reasoning 4, which are shown in Table 6.

Table 6. Propositional symbols of preconditions for Reasoning 4

Symbol	Meaning
s	$LF_{TSfBC,2}$ is given
t	$\tilde{t}_{TSfBC,2}$ is given
u	pixels included in positive areas of $\tilde{t}_{TSfBC,2}$ ($\tilde{t}_{TSfBC,2}^p$) are most probably true tumour positives
v	t_{TSfBC} is given
w	pixels of t_{TSfBC} that are predicted as tumour positives (t_{TSfBC}^p) exist
x	pixels of t_{TSfBC} that are predicted as tumour negatives (t_{TSfBC}^n) exist

- y* the intersection of pixels included in t_{TSfBC}^p and pixels included in $\tilde{t}_{TSfBC,2}^p$ can be considered as most probably predicted true tumour positives
 - z* the intersection of pixels included in t_{TSfBC}^n and pixels included in $\tilde{t}_{TSfBC,2}^p$ can be considered as most probably predicted false tumour negatives
 - a* the intersection of pixels included in t_{TSfBC}^p and pixels included in $\tilde{t}_{TSfBC,2}^p$ can be considered as logically true positives
 - b* the intersection of pixels included in t_{TSfBC}^n and pixels included in $\tilde{t}_{TSfBC,2}^p$ can be considered as logically false negatives
 - c* the intersection of pixels of t_{TSfBC} that are predicted as tumour positives (t_{TSfBC}^p) and pixels included in positive areas of $\tilde{t}_{TSfBC,2}$ ($\tilde{t}_{TSfBC,2}^p$) can be considered as logically true positives
 - d* the intersection of pixels of t_{TSfBC} that are predicted as tumour negatives (t_{TSfBC}^n) and pixels included in positive areas of $\tilde{t}_{TSfBC,2}$ ($\tilde{t}_{TSfBC,2}^p$) can be considered as logically false negatives
-

Thirdly, referring to Table 6, we signify the propositional formalizations of the preconditions 1-9 for Reasoning 4 and Reasoning 4 via the propositional connectives listed in Table 1 as follows.

- | | |
|---|--------------|
| 1) $s \rightarrow t$ | Precondition |
| 2) $t \rightarrow u$ | Precondition |
| 3) $v \rightarrow (w \wedge x)$ | Precondition |
| 4) $(u \wedge w) \rightarrow y$ | Precondition |
| 5) $(u \wedge x) \rightarrow z$ | Precondition |
| 6) $y \rightarrow a$ | Precondition |
| 7) $z \rightarrow b$ | Precondition |
| 8) $a \rightarrow c$ | Precondition |
| 9) $b \rightarrow d$ | Precondition |
| $(v \wedge s) \rightarrow (c \wedge d)$ | Reasoning 4 |

Fourthly, we show the validity of Reasoning 4 via the rules for proof of propositional logical reasoning listed in Table 2 as follows.

$\therefore (v \wedge s) \rightarrow (c \wedge d)$

- | | |
|------------------|-----------------|
| 10) $v \wedge s$ | Hypothesis |
| 11) v | 10); $\wedge -$ |

12) s	10); $\wedge -$
13) $s \rightarrow u$	1),2); HS
14) u	13),12); MP
15) $w \wedge x$	3),11); MP
16) w	15); $\wedge -$
17) x	15); $\wedge -$
18) $u \wedge w$	14),16); $\wedge +$
19) $(u \wedge w) \rightarrow a$	4),6); HS
20) $u \wedge x$	14),17); $\wedge +$
21) $(u \wedge x) \rightarrow b$	5),7); HS
22) $(u \wedge w) \rightarrow c$	19),8); HS
23) $(u \wedge x) \rightarrow d$	21),9); HS
24) c	22),18); MP
25) d	23),20); MP
26) $c \wedge d$	24),25); $\wedge +$
27) $(v \wedge s) \rightarrow (c \wedge d)$	10)-26); Conditional Proof

Since the hypothesis $v \wedge s$ of the 10) step has been fulfilled by the prediction of the image semantic segmentation model for tumour segmentation for breast cancer (t_{TSfBC}) in section 5.2.3 and the two narrated logical facts $LF_{TSfBC} = \{LF_{TSfBC,1}, LF_{TSfBC,2}\}$ Reasoning 4 is proved to be valid.